Contrib Mineral Petrol (1987) 95:4–20

Contributions to Mineralogy and Petrology

Paricutin re-examined: a classic example of crustal assimilation in calc-alkaline magma

A.R. McBirney [1], H.P. Taylor [2], and R.L. Armstrong [3]

[1] Center for Volcanology, University of Oregon, Eugene, OR 97403, USA
[2] Division of Geological and Planetary Sciences, California Institute of Technology, Pasadena, CA 91125, USA
[3] Department of Geological Sciences, University of British Columbia, Vancouver, BC, V6T2B4, Canada

Abstract. Following its birth on the 20th of February 1943, the Mexican volcano Paricutin discharged a total of 1.38 km^3 of basaltic andesite and andesite before the eruption came to an end in 1952. Until 1947, when 75% of the volume had been erupted, the lavas varied little in chemical or isotopic composition. All were basaltic andesites with 55 to 56% SiO_2, $\delta^{18}O$ of +6.9 to 7.0, and $^{87}Sr/^{86}Sr$ ratios close to 0.7038. Subsequent lavas were hypersthene andesites with silica contents reaching 60%, $\delta^{18}O$ values up to +7.6, and $^{87}Sr/^{86}Sr$ of 0.7040 to 0.7043. The later lavas were enriched in Ba, Rb, Li, and K_2O and depleted in MgO, Cu, Zn, Cr, Ni, Sr, and Co. The isotopic and other chemical changes, which appeared abruptly over a few months in 1947, are interpreted as the result of tapping a sharply zoned and density stratified magma chamber. Xenoliths of partially fused felsic basement rocks in the lavas have silica contents greater than 70%, $\delta^{18}O$ of +5.6 to 9.9 and $^{87}Sr/^{86}Sr$ between 0.7043 and 0.7101. In many respects they resemble samples of basement rocks collected from nearby outcrops. Three analysed samples of the latter have silica contents of 65 to 67%, $\delta^{18}O$ of +7.7 to 8.6, and $^{87}Sr/^{86}Sr$ between 0.7047 and 0.7056.

These new data provide strong support for the original interpretations of Wilcox (1954), who explained the chemical variations by a combination of fractional crystallization and concurrent assimilation of up to 20 weight % continental crust. Except for a few trace elements, particularly Ba, Sr, and Zr, the chemical and isotopic compositions of the xenoliths and basement rocks that crop out nearby match the type of contaminant required to explain the late-stage lavas. Some of the discrepancies may be explained by postulating a contaminant that was older and richer in Ba, Sr, and Zr than those represented by the analysed xenoliths. Others can be attributed to chemical changes accompanying disequilibrium partial melting, contact metamorphism, and meteoric-hydrothermal alteration of the country rock. Many of the xenoliths show evidence of having been affected by such processes.

The lavas were erupted from a zoned magma chamber that had differentiated by liquid fractionation prior to the eruption. The order of appearance of the lavas can be explained in terms of withdrawal of stratified liquids of differing densities and viscosities.

Offprint requests to: A.R. McBirney

Introduction

The birth of Paricutin Volcano in Michoacan, Mexico, on the 20th of February, 1943, was followed by nine years of essentially uninterrupted discharge of calc-alkaline magma. During that time, over a cubic kilometer of lava and scoria were erupted, first as olivine-bearing basaltic andesite with a silica content of about 55% and finally as hypersthene andesite with slightly more than 60% SiO_2. The lavas discharged during the first three years contained sporadic xenoliths of leucocratic igneous rocks in all stages of refusion, and the compositional variations of the lavas seemed to be in some way related to assimilation of these sialic crustal rocks. Samples collected at successive stages of the eruption provide an extraordinary opportunity to examine the degree to which assimilation of felsic crust in a differentiating basaltic magma can lead to andesitic compositions. Moreover, the systematic variations found in the lavas afford an unusually instructive example of a type of compositional zoning that seems to be an important feature of calc-alkaline differentiation.

The initial study of the rocks by Wilcox (1954) utilized the optical and chemical techniques available at that time to calculate a chemical and thermal balance for the principal components of the system. In so doing, Wilcox found the compositional variations to be consistent with addition of 25.4 g of average xenolithic material and concurrent subtraction of 2.9 g of olivine (Fo 80) and 9.6 g of plagioclase (An 70) from 100 grams of the earliest liquid to yield 112.9 g of a derivative liquid approximating the composition of the groundmass of the last lava erupted. The heat released by crystallization of the olivine and plagioclase would fall short of that required to melt the xenoliths, but it seemed reasonable to assume that additional heat could be supplied by convection from a deeper source and crystallization of unseen magma. The quantitative nature of the mass-balance calculation, based as it was on field and petrographic evidence, seemed to offer a convincing model for the origin of andesites in general.

More recently, as studies of trace elements and isotopic ratios provided additional means of evaluating assimilation, petrologists began to question whether wholesale incorporation of crustal material was a significant factor in the origin of andesites. For example, early measurements of the strontium isotopic ratios of Paricutin rocks (Tilley et al.

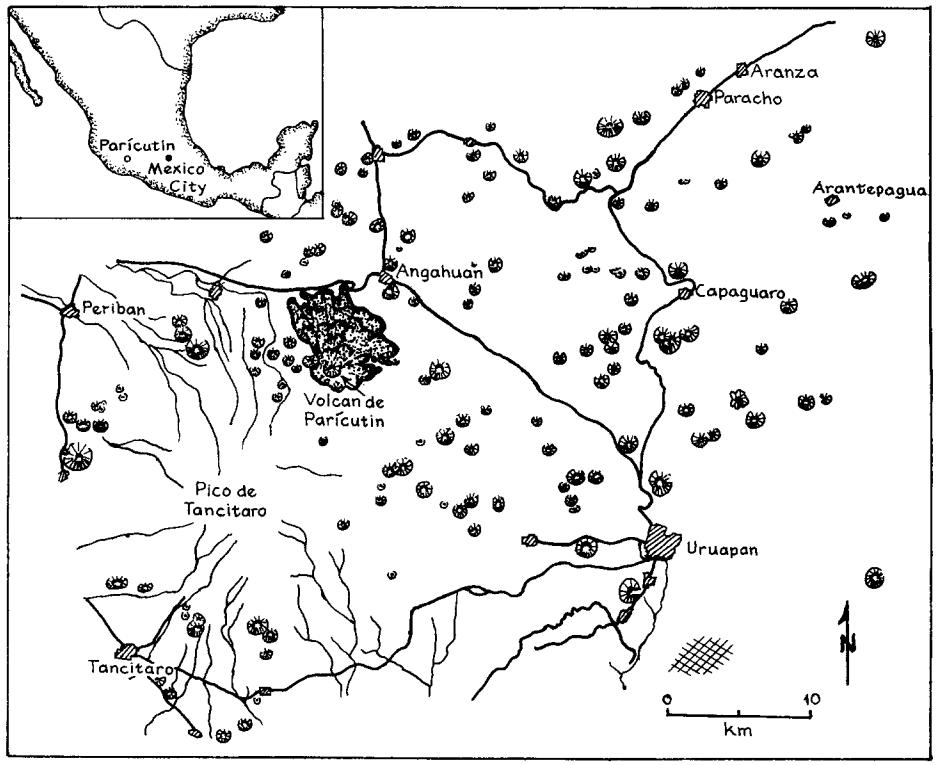

Fig. 1. Sketch map of the Paricutin region showing the distribution of youthful cones. All of the vents produced basalt or basaltic andesite. *Cross-hatched pattern* indicates area of exposures of basement rocks (after Williams 1950)

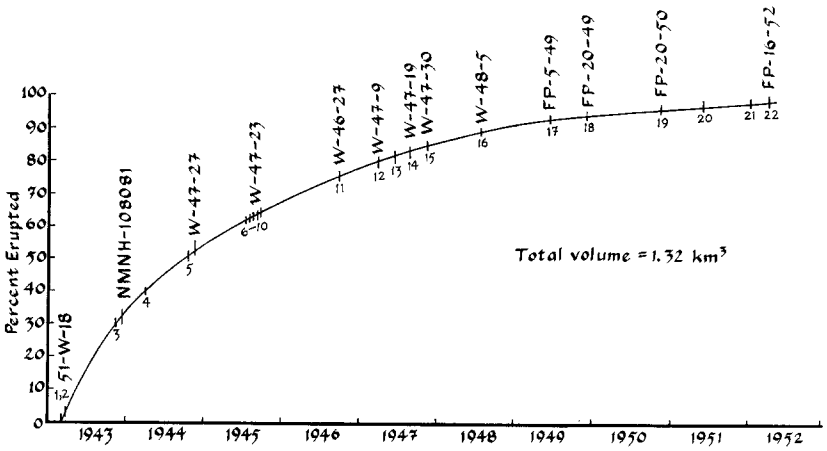

Fig. 2. Cumulative volume of lava and cinders erupted during the life of Paricutin Volcano. Mass has been recalculated to volumes assuming a uniform density of 2.6 (after Fries 1953). Numbers *1* through *22* indicate original samples of Wilcox (1954). Numbers of samples used here are indicated above the curve

1968) raised doubts that assimilation had contributed materially to the observed compositional changes. It seems appropriate, therefore, to utilize these new geochemical tools to re-examine the suite of Paricutin lavas in greater detail and to reconsider the mechanisms responsible for their compositional variations.

Full accounts of the history of the eruption and petrographic descriptions of the lavas and xenoliths can be found in the original study (Wilcox 1954) and in other reports cited in the same paper. For our present purposes, it will suffice to summarize the essential elements of the eruption and salient petrographic features of the rocks.

The eruption

Paricutin is one of nearly 200 monogenetic volcanoes scattered in seemingly random fashion over an area of about 1,500 km^2 (Fig. 1) in the western part of the Trans-Mexican Volcanic Belt. The area is underlain by Mesozoic plutonic rocks, which are exposed at the edge of the Paricutin Plateau about 30 km to the southeast and were found as inclusions in the lavas and pyroclastic ejecta of the volcano.

The initial outbreak on 20 February, 1943, was preceded by several weeks of local earthquakes that increased in intensity before ending abruptly with the first discharge of gas-rich magma. The vent opened as a dilational fracture crossing a flat area that does not seem to have been the scene of previous activity. The cone grew rapidly at first; at the end of two weeks it had reached a height of 165 m and measured 560 m across its base. Subsequent growth became slower as the rate of eruption of pyroclastic ejecta declined and lava began to issue from a fissure at the northeastern base of the cone. Thereafter, the discharge of lava varied in rate and shifted from one part of the fissure to another, but at no time was it observed to cease altogether. The average rate of discharge declined gradually after the first year (Fig. 2). In all, the volcano erupted 3,596 million t of lava and cinders which, if converted to a liquid having a density of 2.6, would amount to about 1.38 km^3 of magma (Fries 1953).

Gas separated from the eruptive column somewhere in the upper levels of the vent, so that fumes of water vapor, sulfur gases, and carbon dioxide continued to be emitted from the crater while

Table 1. Major- and trace-element compositions of Paricutin lavas. See text and appendix for sources of samples and methods of analyses

Sample no.	51-W-18	108081	W-47-27	W-47-23	W-46-27	W-47-9	W-47-30	W-48-5	FP-5-49	FP-20-49	FP-20-50	FP-16-52
Year erupted	1943	1944	1944	1945	1946	1947	1947	1948	1949	1949	1950	1952
Cumulative vol.	1%	33%	51%	64%	75%	78%	82%	85%	93%	94%	97%	100%
SiO_2	54.59	55.39	55.71	55.79	56.13	57.05	58.39	59.09	59.41	59.77	60.24	60.07
TiO_2	0.99	0.94	1.01	0.90	1.02	0.89	0.86	0.78	0.84	0.83	0.80	0.81
Al_2O_3	17.83	17.64	17.24	17.48	17.34	17.27	17.78	17.55	17.30	17.29	17.30	17.28
Fe_2O_3	2.01	2.16	2.06	1.83	1.74	1.42	1.87	2.04	1.57	1.21	1.19	1.37
FeO	5.43	5.46	5.48	5.30	5.42	5.21	4.51	4.27	4.78	4.95	4.59	4.39
MnO	0.12	0.13	0.13	0.12	0.12	0.12	0.12	0.11	0.11	0.11	0.10	0.10
MgO	5.44	5.43	5.61	5.75	5.58	5.64	4.03	4.03	3.81	3.72	3.55	3.73
CaO	7.25	7.18	6.98	6.81	6.99	6.94	6.75	6.46	6.36	6.28	6.14	6.16
Na_2O	3.95	3.98	3.99	3.81	3.79	3.71	3.86	3.92	3.71	3.74	4.01	4.00
K_2O	0.91	1.15	1.18	1.19	1.30	1.23	1.30	1.50	1.67	1.67	1.66	1.67
H_2O+	0.16	0.09	0.20	0.20	0.20	0.17	0.11	0.08	0.12	0.12	0.04	0.03
H_2O-	0.04	0.05	0.06	0.10	0.06	0.02	0.01	0.03	0.01	0.00	0.04	0.05
P_2O_5	0.27	0.35	0.33	0.30	0.36	0.29	0.30	0.30	0.31	0.31	0.29	0.28
Total	98.99	99.95	99.98	99.58	100.05	99.96	99.89	100.16	100.00	100.00	99.95	99.94
Ba	315	376	388	440	413	435	436	506	549	597	558	604
Sr	607	578	596	537	588	580	575	556	540	512	533	541
Li	12	14	16	15	16	16	19	19	20	21	20	20
Rb	14	15.4	18	13.4	15	16.8	23.2	24.6	26.3	22.2	24.6	27
Cs	nd	nd	0.22	0.37	0.36	0.54	0.52	0.60	0.53	0.55	0.63	0.66
Sc	17.33	16.6	16.45	17.02	17.12	16.19	15.03	15.05	14.45	14.41	14.41	13.76
Cr	144.7	176	155.2	170	152.7	162.4	78.5	88	75	67.8	66.5	76
Co	35	33	32	27	29.7	24.7	20.5	20.1	18.7	18.7	21.5	18.1
Ni	116	103	126	127	122	126	71	73	60	57	55	63
Cu	168	37	172	123	39	37	nd	34	34	36	37	34
Zn	140	85	230	130	80	73	75	76	76	75	76	72
Zr	116	171	174	147	167	150	160	164	175	162	174	173
Hf	2.94	3.3	3.57	3.66	3.57	3.44	3.53	3.99	3.93	3.96	4.10	3.84
Ta	0.38	nd	0.60	0.56	0.58	0.52	0.48	0.51	0.55	0.48	0.50	0.49
Th	0.94	1.42	1.62	1.54	1.69	1.51	1.49	1.76	1.74	1.77	1.87	1.91
U	nd	0.9	nd	0.70	nd	nd	nd	nd	nd	nd	nd	nd
La	13.1	16	18.1	16.9	17.6	15.6	17.0	18.6	19.1	19.6	19.5	19.6
Ce	29.6	35.7	38.9	40.4	39.6	35.9	36.5	41.4	40.5	43.0	43.4	40.9
Nd	20.6	24	24.0	25.0	21.0	13.6	nd	nd	29.0	24.0	21.0	24.6
Sm	3.8	4.5	4.6	4.2	4.4	4.0	4.1	4.2	4.2	4.5	4.4	4.3
Eu	1.32	1.39	1.41	1.36	1.44	1.27	1.34	1.45	1.34	1.33	1.35	1.29
Tb	0.67	0.62	0.69	0.72	0.72	0.61	0.64	0.68	0.65	0.68	0.67	0.64
Yb	1.79	2.2	2.06	1.88	1.84	1.73	1.73	2.09	1.96	1.95	1.72	1.78
Lu	0.28	0.29	0.31	0.31	0.31	0.28	0.28	0.29	0.28	0.31	0.29	0.28

degassed a lava poured from a lateral vent near the base of the cone (Krauskopf 1948). Volatiles were most abundant in the opening stages of the eruption but declined abruptly and remained low to moderate until the final weeks when a brief burst of increased discharge marked the closing phase of activity.

Petrography of lavas and xenoliths

The most notable petrographic features of the lavas, apart from their xenoliths, are, first, the small size and scarcity of phenocrysts of plagioclase and augite, and, second, the crystallization of hypersthene in place of olivine as the magma became more siliceous. The first lavas erupted in 1943 and 1944 contained small phenocrysts of plagioclase and olivine. The olivine, Fo 79, amounted to 2 to 4% of the volume and reached a maximum dimension of about 0.5 mm, while plagioclase, An 59, up to 0.4 mm in length, accounted for, at most, 2% of the volume. No clear division in size separates these phenocrysts from seriate olivine and plagioclase crystals in the groundmass.

Plagioclase occurred only as microphenocrysts in lavas erupted after mid-1944. Olivine phenocrysts seem to have been slightly more abundant in the lavas of 1946 and early 1947, but after the end of 1945 they were rimmed with pyroxene and by mid-1948 olivine had all but disappeared. Its place was taken by hypersthene, En 72–80, which became increasingly abundant after the end of 1946. Augite is present as microphenocrysts in some early lavas but is confined to the groundmass after 1945. A few crystals of opaque spinel are seen in the early lavas but are volumetrically insignificant.

Xenoliths seem to have been most common in bombs erupted during the first years of activity. With the exception of a fragment in the core of a bomb erupted in June, 1947, and another in lava erupted in October of 1949, the xenoliths known to have been collected were from lavas erupted in the first three years of activity. All are fragments of siliceous igneous rocks, but, owing to their wide range of alteration and fusion, few samples can be identified with certainty. Granite, granodiorite, and quartz monzonite seem to have been most common, but a few fragments were identified as porphyritic hypabyssal or effusive rocks of dacitic or rhyolitic composition.

Most xenoliths consist of highly vesicular glass with rounded grains of quartz and fritted feldspar and lesser amounts of ferro-

magnesian minerals in advanced stages of alteration. The least altered specimens still preserve coarse granitic textures, but even these have intergranular glass. A typical quartz monzonite, for example, consists of anhedral grains of fractured and cloudy orthoclase and albitic plagioclase, about 20% quartz, and about 15% opaque material derived, no doubt, from breakdown of ferro-magnesian minerals. Accessory minerals include sphene, zircon, and apatite. Apart from alteration and different proportions of feldspars, the rock is not unlike the granodioritic rocks that crop out 30 km to the southeast.

Petrographic evidence of contamination of the magma by these xenolithic rocks is far from obvious. Xenocrysts, reversely zoned or resorbed feldspar, or other signs of inhomogeneity or disequilibrium are rare. If foreign material was dispersed through the magma in the amount required to account for the observed compositional changes, it was so thoroughly assimilated that it left little visible trace of its contribution.

Major-element chemistry

Lavas

We have reanalysed fragments from most of Wilcox's (1954) twenty-two hand-specimens of lavas, and with the possible exception of Al_2O_3, which is slightly less abundant in some of our analyses, we find no differences between the original data and new determinations. All the major-element data given in Table 1 and Fig. 3 are taken from the original analyses with the exception of sample 108081, which is a new analysis of a sample that was generously provided by the National Museum of Natural History.

The most notable feature of the major elements is the sharp increase of SiO_2 and the corresponding decrease of MgO in the late stages of the eruption. CaO and total iron (as FeO) declined slightly, K_2O increased, and other components remained nearly constant. The most marked change occurred in early 1947, by which time about 80% of the total volume had been erupted. At that time, alumina, which declined slightly in the early stages, began to increase and continued to do so until late 1947 when 85% of the volume had been discharged; it then reversed this trend and declined until the eruption ended. Marked inflections are also found in trace-element abundances of the lavas erupted during this same interval.

The major-element variations can be related to mineralogical components by plotting the compositions on a CMAS diagram of the type devised by Cawthorne and O'Hara (1976) and shown here as Fig. 4. The experimentally determined field boundaries of olivine, amphibole, orthopyroxene, and plagioclase are based on rocks of other compositions. Because these boundaries are strongly affected by sodium content, water pressure, and other factors, they have been adjusted to correspond to the observed chemical trends and mineral assemblages in the Paricutin rocks.

Figure 4 reveals an inflection in the compositional trend at an early stage when 40 to 50% of the volume had been erupted. The change is consistent with early fractionation of olivine until the liquid reached the stability field of amphibole. Orthopyroxene would have begun to crystallize at the time of the more pronounced change in 1947, and phenocrysts of hypersthene were in fact observed to appear in the lavas at that stage.

The change that occurred later in 1947, after about 85% of the volume had been discharged, corresponds to a stage at which the phase diagram indicates the liquid would have

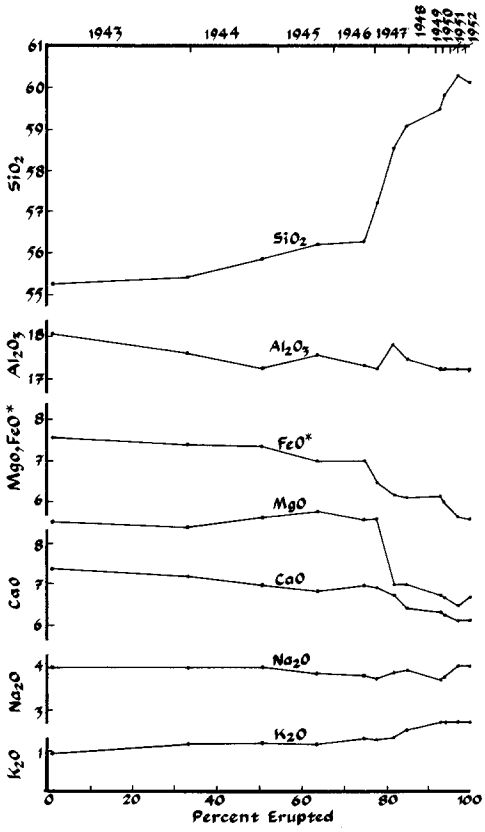

Fig. 3. Variations of major elements in Paricutin lavas plotted as a function of cumulative volume erupted

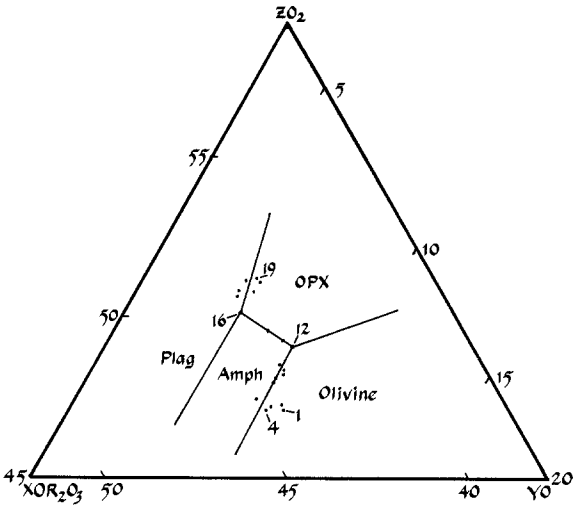

Fig. 4. CMAS diagram showing compositional variations of Paricutin lavas in relation to the inferred stability fields of mineral phases determined for calc-alkaline rocks by Cawthorn and O'Hara (1976). Phase boundaries have been adjusted to fit the observed trends of Paricutin lavas. Numbers correspond to samples shown in Fig. 2. ZO_2 is essentially SiO_2 less alkalies, XOR_2O_3 is mostly CaO, Al_2O_3 and alkalies, and YO is the sum of MgO and FeO*. Proportions are in mole percent. For more information on methods of plotting see: Cox KG, Bell JD, Pankhurst RJ (1979) The interpretation of igneous rocks. Allen Unwin, London, p 415

just begun to crystallize plagioclase, and yet plagioclase is present as phenocrysts in even the earliest lavas and is seen only as microphenocrysts after about half the magma had been discharged. These differences between the observed assemblages in lavas and those predicted by the phase dia-

Table 2a. Major- and trace-element analyses of xenoliths

	51-W-1	51-W-5	51-W-6	51-W-7	51-W-8	51-W-9	51-W-10	51-W-11	51-W-22	108124	108126	108132	AVE.
SiO_2	70.88	71.99	72.61	71.00	75.95	70.88	73.64	74.57	71.37	72.40	71.93	70.80	72.63
TiO_2	0.36	0.21	0.17	0.18	0.04	0.36	0.04	0.04	0.19	0.21	0.23	0.39	0.20
Al_2O_3	14.27	15.95	14.98	14.83	13.51	14.38	12.07	13.58	15.19	15.66	14.98	14.58	14.56
Fe_2O_3	1.52	0.68	0.55	0.64	0.25	1.51	0.26	0.41	0.53	0.66	0.80	0.80	0.72
FeO	1.53	1.22	1.51	1.43	0.27	1.59	0.51	0.32	1.38	1.38	1.25	1.40	1.15
MnO	0.05	0.05	0.06	0.06	0.03	0.05	0.02	0.01	0.04	0.06	0.06	0.05	0.05
MgO	1.17	0.71	0.32	0.53	0.05	1.25	3.44	0.46	0.63	0.53	0.55	1.13	0.90
CaO	1.65	2.49	2.96	3.13	1.05	2.93	4.14	1.14	2.55	3.14	2.79	3.46	2.63
Na_2O	4.18	4.03	4.75	4.13	3.90	3.32	2.41	4.15	3.99	4.80	4.67	3.36	3.99
K_2O	3.64	2.43	1.63	2.38	4.74	3.90	2.73	4.67	2.76	1.49	2.15	3.69	3.03
H_2O+	0.11	0.13	0.39	0.47	0.13	0.14	0.41	0.42	0.32	0.13	0.19	0.11	–
H_2O-	0.05	0.02	0.07	0.11	0.01	0.01	0.11	0.08	0.03	0.05	0.03	0.07	–
P_2O_5	0.08	0.09	0.16	0.19	0.02	0.06	0.06	0.01	0.32	0.21	0.27	0.08	0.13
Total	99.49	100.00	100.16	99.08	99.95	100.38	99.84	99.86	99.30	100.72	99.90	99.92	99.99
Ba	371	–	288	767	76	612	217	112	2097	289	297	508	512.2
Sr	78	–	404	452	35	186	213	44	382	547	456	167	269.5
Li	29	–	16	15	5	20	13	5.7	9	14	15	20	14.7
Rb	153	–	36	82	139	197	148	87	63	33	52	169	105.4
Cs	2.5	–	1.1	–	2.6	–	–	–	–	–	–	–	2.1
Sc	7.8	–	2.6	2.8	2.1	–	–	–	–	2.7	2.8	8.1	4.1
Ni	–	–	18	–	–	35	7.2	27	10	8.2	11	26	17.8
Cr	18	–	15	37	10	18	88	19	9	5.3	4.7	12	21.4
Co	6.5	–	2.3	–	–	4.3	tr	tr	tr	0.4	2.7	7.1	3.9
Cu	26	–	7.3	18	22	13	49	3.7	61	51	44	37	30.2
Zn	41	–	47	52	16	34	37	15	38	56	50	31	37.9
Ta	0.05	–	0.4	–	0.5	–	–	–	–	–	–	–	0.5
Zr	136	–	110	–	56	154	–	68	175	141	135	137	123.6
Hf	4.0	–	2.9	2.8	3.1	–	–	–	–	3.0	2.7	4.4	3.3
U	4.2	–	0.6	–	3.3	–	–	–	–	–	–	–	2.7
Th	21.2	–	1.7	1.7	7.2	–	–	–	–	1.7	1.6	18.2	7.6
La	14.5	–	14.7	16	3.9	–	–	–	–	13	13	20	13.6
Ce	28.6	–	28.6	27.3	11.2	–	–	–	–	25.6	26.8	40	26.9
Nd	12.2	–	–	9	7.4	–	–	–	–	10	10.1	13	10.3
Sm	3.1	–	1.8	1.9	2.1	–	–	–	–	1.8	1.9	3.5	2.3
Eu	0.59	–	0.56	0.66	–	–	–	–	–	0.52	0.49	0.60	0.57
Tb	0.39	–	0.21	0.25	0.65	–	–	–	–	0.19	0.25	0.70	0.37
Yb	1.40	–	0.84	0.86	2.56	–	–	–	–	0.94	0.94	2.06	1.37
Lu	0.31	–	0.14	0.14	0.43	–	–	–	–	0.137	0.144	0.35	0.24

Table 2b. Comparison of the composition of the glassy fraction and bulk composition of a partially melted xenolith (51-W-10). The composition of the glass is an average of six microprobe analyses which have the standard deviations shown under "S.D". The total for the average composition of glass (98.12%) does not include water, which would amount to 1.04% if all the water in the bulk sample (0.52%) is in the glass and the sample is 50% melted. Most of the remaining deficiency (0.84%) can be attributed to oxidation of iron, trace elements, and possibly volatilization of sodium. Also shown are average compositions and standard deviations for the bulk compositions of twelve xenoliths and three basement rocks from Table 2a and c

	Bulk rock	Glass		Bulk xenoliths		Basement	
		Aver.	S.D.	Aver.	S.D.	Aver.	S.D.
SiO_2	73.64	77.29	1.99	72.34	1.64	67.47	2.71
TiO_2	0.04	0.03	0.02	0.20	0.12	0.70	0.13
Al_2O_3	12.07	12.22	1.10	14.50	1.06	13.46	1.19
FeO*	0.69	0.76	0.16	1.79	0.79	4.92	0.58
MnO	0.02	0.04	0.03	0.04	0.02	0.15	0.05
MgO	3.44	0.10	0.03	0.90	0.88	2.15	0.53
CaO	4.14	1.48	0.56	2.62	0.89	4.00	0.41
Na_2O	2.41	0.60	0.67	3.97	0.68	3.30	0.00
K_2O	2.73	5.59	0.30	3.02	1.10	3.66	0.48
P_2O_5	0.06	0.01	0.01	0.13	0.10	0.07	0.01

Table 2c. Major- and trace-element analyses of samples from exposures of basement rocks about 30 km southeast of Paricutin

	FP-20-52	FP-26-52	FP-27-52	AVE.
SiO_2	65.40	67.43	67.07	67.47
TiO_2	0.73	0.61	0.79	0.70
Al_2O_3	14.44	13.78	12.32	13.46
Fe_2O_3	2.40	1.95	1.30	1.84
FeO	3.25	2.60	3.81	3.26
MnO	0.16	0.18	0.09	0.15
MgO	2.56	1.62	2.12	2.15
CaO	5.07	3.73	4.42	4.00
Na_2O	3.40	3.20	3.31	3.30
K_2O	3.25	4.09	3.65	3.66
H_2O+	0.51	0.51	0.31	–
H_2O-	0.27	0.47	0.18	–
P_2O_5	0.14	0.11	0.08	0.07
Total	101.58	100.28	99.45	100.00
Ba	564	607	515	562
Sr	202	186	166	185
Li	28	24	28	27
Rb	123	195	170	163
Cs	4.2	–	–	4.2
Sc	18.0	11.9	14.7	14.9
Ni	18	11.6	57	28.9
Cr	49	13	35	32.3
Co	73	50	57	60
Cu	20	49	47	38.7
Zn	101	120	82	101
Zr	241	244	242	242.3
Hf	6.7	–	–	6.7
Ta	2.6	–	–	2.6
Th	11.8	11.9	14.7	12.8
U	4.5	5.0	3.9	4.5
La	19.3	20	21	20.1
Ce	37.0	40	47	41.3
Nd	28.8	16	21	21.9
Sm	4.7	4.7	5.2	4.9
Eu	0.8	0.8	0.8	0.8
Tb	0.8	0.6	0.8	0.7
Yb	2.75	2.8	3.1	2.9
Lu	0.43	0.45	0.44	0.44

gram can be reconciled, at least in part, by Eggler's experimental evidence (1972) that amphibole was stable at depth but disappeared as the magma rose to shallower levels. While amphibole has not been seen in the Paricutin rocks, it is found in the lavas of several nearby volcanoes in the Paricutin region (Williams 1950).

Osborne and Rawson (1980) found magnetite to be a near-liquidus phase at oxygen fugacities near the Ni-NiO buffer, a water content of 2%, and total pressures between 1 and 10 kb, but phenocrysts of iron oxides are very rare in the lavas, and, as will be seen in a later section, do not seem to have affected the compositional evolution of the rocks.

The early appearance of plagioclase and the absence of augite is easy to account for if it is postulated that a loss of water during ascent caused the cotectic to shift away from plagioclase and toward augite (Yoder 1969). The smaller size of plagioclase crystals in late-stage lavas may be due to the greater silica content of the liquid and the slower rates of nucleation and growth of crystals that would accompany an increase in viscosity. Another factor may have been the greater concentration of water in the upper part of the reservoir.

Xenoliths and basement rocks

Because of the broad compositional range and differing degrees of melting of the xenoliths, it is difficult to arrive at a single composition that might be representative of the basement material incorporated into the Paricutin magma. Wilcox (1954) provided major-element analyses of four typical xenoliths, and we have obtained eight new analyses for a somewhat greater range of compositions, but the effect of these additional analyses on the calculated average compositions is not great (Table 2a). Three new analyses of samples of unaltered basement rocks from outcrops about 30 km from Paricutin differ somewhat from the average xenolith (Table 2b, c), but there is no way of knowing how representative these distant outcrops are of rocks immediately under the volcano.

Three xenoliths with differing proportions of glass were analysed in bulk to see if any trend could be related to progressive melting. One of these (51-W-1) is dense and contains only about 10% glass; a second (51-W-6) is slightly vesiculated and contains about 50% glass, and the third (51-W-8), a very frothy sample, has about 90% glass. The analyses show no discernible trend that would indicate that individual components were gained or lost during melting, but we cannot be certain that the original compositions of the xenoliths have been preserved.

We have also obtained microprobe analyses of the glassy fraction of a partly fused xenolith (Table 2b). When compared with the bulk composition of the same rock, the glass is seen to be richer in SiO_2 and K_2O and poorer in Na_2O, MgO, and CaO. Its composition indicates that a potassium-rich mineral, probably biotite, was among the first phases to break down and that rapid melting caused the composition of the liquid to diverge from that expected under equilibrium conditions.

Volatile content

Estimates of the volatile content of the magma have been uniformly low. Fries (1953) calculated the amount of gases released in the fume cloud to be slightly more than one percent by weight of the lava. This is much less than the estimate of Eggler (1972), who concluded from experimental studies of phase relations that the Paricutin magma contained about 2.2 weight % water when it was in equilibrium with its phenocrysts at a temperature of 1,110° C and more than 10 kb total pressure. Water could, of course, have been exsolved during ascent of the magma and might not be represented in the fume clouds observed by Fries. Anderson (1974) estimated a "before eruption" water content of about 1.5 weight % from the compositions of glass inclusions. He also noted (Anderson 1979) that the Cl/K_2O ratio declined from 0.072 in glass trapped in phenocrysts to 0.05 in glass surrounding the crystals. He attributed this difference to a loss of chlorine along with about 1.0 weight % water between the depth at which the phenocrysts grew and a shallower level where the magma re-equilibrated at lower pressures. His results are consistent with those of Eggler and Fries and lend support to the conclusion that the magma lost about half of its volatile content enroute to the surface. As already noted, the fact that the rocks

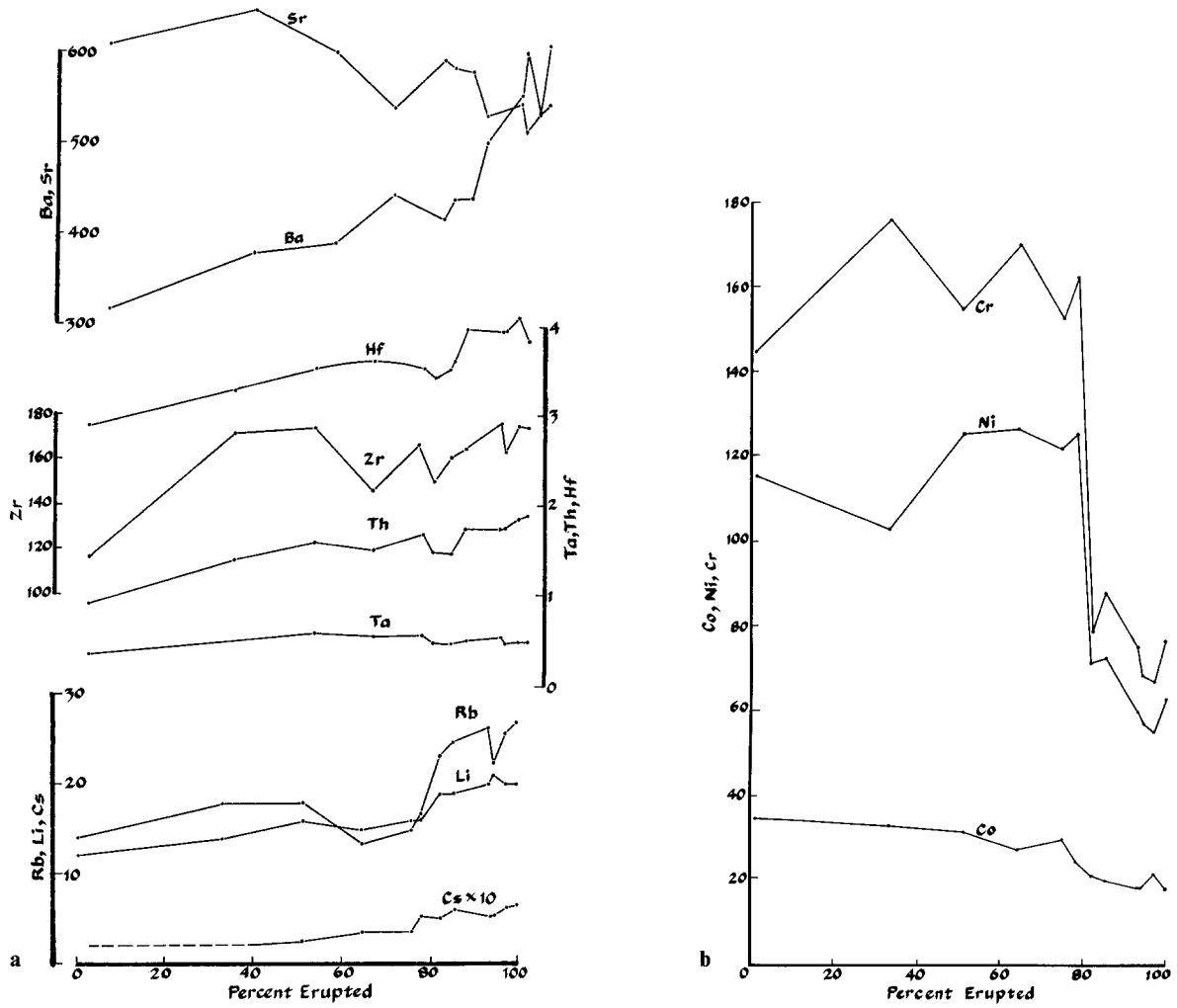

Fig. 5a, b. Variations of trace elements in Paricutin lavas plotted against cumulative volume of magma erupted. All values are in ppm

do not have a Ca-rich pyroxene on their liquidus could be attributed to a loss of water after they had differentiated.

Trace elements

The lavas, xenoliths, and basement rocks have been analysed for most trace element of petrologic interests. Zr, Rb, Ni, and Sr were measured by X-ray fluorescence, Ba, Sr, Rb, Co, Cr, Cu, Zn, and Li by atomic absorption or flame emission, and Sc, Hf, Ta, Th, U, Cs, and the rare-earth elements by neutron activation. These data are compiled in Tables 1 and 2a, c and are illustrated graphically in Fig. 5.

Lavas

The abundances of most trace-elements in the lavas changed only moderately as the magma evolved. A few, most notably Ba, Rb, Ni, and Cr, show a marked change around mid 1947 when about 80% of the total volume had been discharged. Except for somewhat erratic Nd values due to poor precision in the analytical determinations, little change in the chondrite-normalized curves is noticeable anywhere in the REE abundances throughout the eruptive sequence (Fig. 6); all lavas have a similar light-REE enriched pattern. The first lava of early 1943 is less enriched in the light REE (La and Ce) than are later lavas.

Xenoliths and nearby basement rocks

Trace elements have a wide range of concentrations in the xenoliths and nearby basement rocks, but the concentrations of certain constituents show that the two suites are not strictly equivalent. Comparisons of the averages in Table 2a, c show the basement rocks to be poorer in SiO_2, Na_2O, and Sr but richer in K_2O, Ba, Li, Rb, all transition metals, Zr, and Sr/Rb. They define a separate group on all the variation diagrams in Fig. 7.

The compositions of analysed xenoliths (Fig. 7) are scattered and for some elements fall far from the projected trend of lavas. This discrepancy is especially clear in the case of Zr, Sr, and Ba, all of which have such low abundances in the xenoliths that they are incompatible with the observed trends in the lavas. The condrite-normalized REE patterns (Fig. 6) for the analysed xenoliths also have a wide range. The basement samples and about half of the xenoliths have a distinct europium anomaly that is not apparent in the lavas. Most are light-REE enriched and have lower REE concentrations than the lavas, but the very frothy xenolith (51-W-8) has a flat pattern that is distinct from

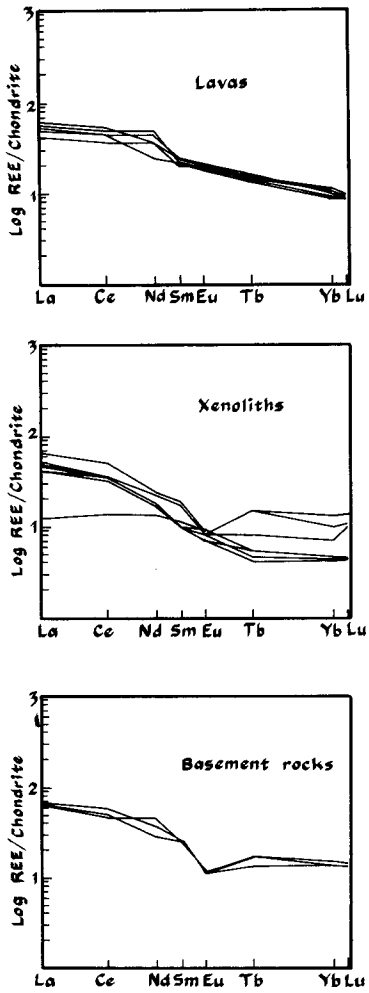

Fig. 6. Rare-earth element distribution patterns for nine selected Paricutin lavas, xenoliths, and basement rocks. Note the absence of europium anomalies in the lavas and the strong enrichment of the light rare earths. Data (from Table 1) have been normalized to chondritic meteorites

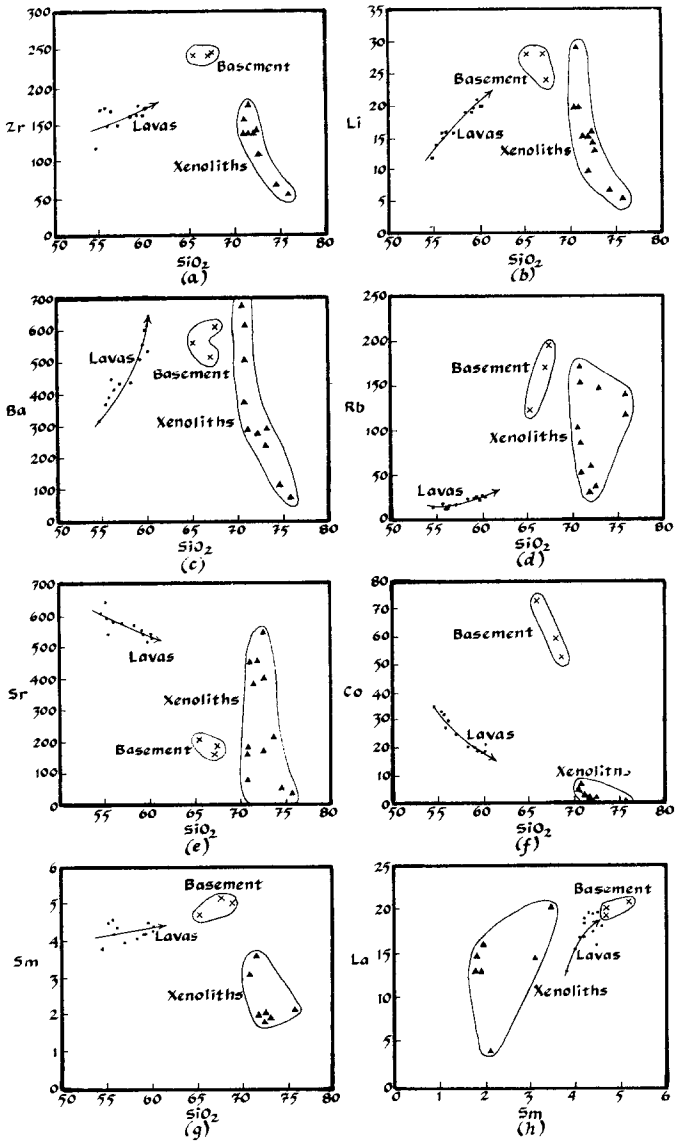

Fig. 7a–h. Trace-element variations in lavas (*dots*) and xenoliths (*triangles*) erupted from Paricutin volcano. For comparative purposes, compositions are also shown for granitic rocks postulated to form the basement under the volcano (*crosses*). Trends of compositional changes in the lava are indicated by *arrows* that are fitted visually through the points. In **c**, the values for Ba in two xenoliths are off the scale of the diagram at 767 ppm Ba, 71.00% SiO_2 and 2,097 ppm Ba, 71.37% SiO_2

that of all other samples. As already noted, this specimen is also unusual in other ways.

Oxygen isotopes

Lavas

$^{18}O/^{16}O$ ratios were determined for 11 lavas and one sample of ash representing the sequence erupted from 1943 to 1952. The data are given in Table 3 and shown graphically in Fig. 8.

The first lavas to erupt have a $\delta^{18}O$ value of +6.9 typical of many basaltic andesites and andesites erupted in island-arcs and active continental margins around the Pacific Ocean. The $\delta^{18}O$ values remained nearly constant at +6.9 to +7.1 up to 1947 but then increased abruptly to +7.5 to 7.7 in the later lavas. Such a change clearly indicates some type of open-system behavior such as assimilation of high-^{18}O material; it cannot be the result of simple closed-system fractional crystallization (Garlick 1966; Taylor 1968, 1977; Matsuhisa et al. 1980; Anderson et al. 1971).

Xenoliths and basement rocks

Most of the analysed xenoliths and nearby basement rocks have $\delta^{18}O$ values of +8.2 to 9.2, distinctly greater than the values that characterize the early lavas. These values are typical of many calc-alkaline granitic rocks throughout the world, and specifically of the great Mesozoic and Cenozoic batholiths around the Pacific margins (e.g. Taylor and Silver 1978; Criss and Taylor 1983; Masi et al. 1981). Thus, as far as the $^{18}O/^{16}O$ systematics are concerned, these xenoliths and basement rocks represent plausible contaminants that could explain the post-1947 ^{18}O-enrichments of the lavas.

Note that most of the xenoliths in the ejecta of 1943 have very high $\delta^{18}O$ values of +9.1 to +9.9, whereas the

Table 3. Oxygen and strontium isotope ratios of Paricutin lavas, ash, xenoliths, and basement rocks

Sample	Date erupted	$\delta^{18}O$	[a]	Rb[b]	Sr[b]	$^{87}Rb/^{86}Sr$	$^{87}Sr/^{86}Sr$
Lavas and ash							
51-W-18	Feb 1943	6.92±0.09	(3)	14	607	0.067	0.7038
108081	Jan 1944	7.03±0.04	(2)	15.4	578	0.077	0.7039
W-47-27	Oct 1944	6.95	(1)	18	596	0.087	0.7038
W-47-23	Sept 1945	7.06±0.08	(2)	13.4	537	0.072	
W-46-27	Sept 1946	7.00±0.12	(3)	15	588	0.074	0.7037
W-47-9	Apr 1947	7.25±0.10	(2)	16.8	580	0.084	0.7041
Ash fall[c]	Nov 1947	7.55±0.17	(2)	–	–	–	0.7043
W-47-30	Nov 1947	7.60	(1)	23.2	575	0.116	0.7040
W-48-5	Sept 1948	7.59	(1)	24.6	556	0.128	0.7041
FP-5-49	May 1949	7.48	(1)	26.3	540	0.141	0.7042
FP-20-49	Dec 1949	7.69±0.06	(2)	22.2	512	0.125	0.7040
FP-20-50	Sept 1950	7.57	(1)	24.6	533	0.134	0.7042
FP-16-52	Feb 1952	7.54±0.04	(2)	27	541	0.143	0.7043
Xenoliths							
51-W-1	1943	9.94±0.01	(2)	153	78	5.68	0.7071
51-W-5	1943	9.44	(1)	–	–	–	0.7044
51-W-6	1943	9.11	(1)	36	404	0.26	0.7043
51-W-7[d]	1944–45	8.21	(1)	82	452	0.53	0.7047
51-W-8[d]	1944–45	5.59±0.01	(2)	139	35	11.49	0.7101
51-W-9	1944–45	8.71±0.00	(2)	197	186	3.07	0.7059
51-W-10[d]	1944–45	6.84	(1)	148	213	2.02	0.7054
51-W-11	1943	6.77	(1)	87	44	5.72	0.7070
51-W-22	1943	9.06±0.20	(2)	63	382	0.48	0.7046
Basement rocks							
FP-20-52	–	8.57±0.06	(2)	123	202	1.75	0.7047
FP-26-52	–	8.54	(1)	195	186	3.02	0.7056
FP-27-52	–	7.66	(1)	170	166	2.96	0.7056

[a] Error is average deviation from the mean; number in parentheses is number of times analysed
[b] Analyses in parts per million by X-ray fluorescence
[c] 3.5 mm ash collected 5 km north of the vent
[d] Frothy pumiceous sample

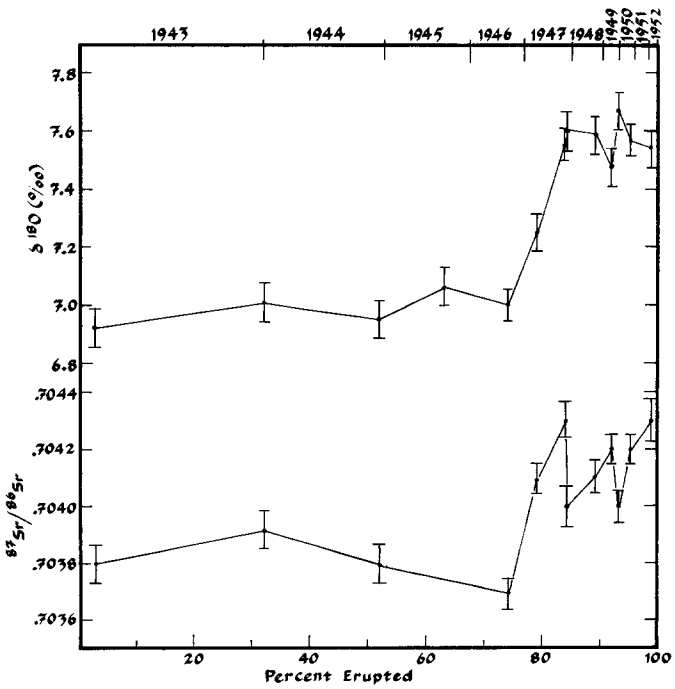

Fig. 8. Plot of $\delta^{18}O$ and $^{87}Sr/^{86}Sr$ in Paricutin lavas against cumulative percent erupted

xenoliths erupted in 1944–45 tend to be lower. One of the latter is particularly frothy and glassy and has a $\delta^{18}O$ value of +5.6, markedly lower than that of the initial Paricutin lava. The low ^{18}O values of frothy or pumiceous xenoliths would be expected if they had high volatile contents, and the most logical interpretation of these data is that such xenoliths were altered and depleted in ^{18}O by meteoric-hydrothermal activity at the margins of the Paricutin magma chamber. The hydrous alteration minerals (chlorite, epidote, etc.) formed by this activity would have been dehydrated when the xenoliths were incorporated in the andesitic magma and the evolved water could promote melting of other phases as well.

Correlation with major- and trace-element compositions

The Paricutin lavas have a good positive correlation between $\delta^{18}O$ and the trace elements Ba, Li, Rb, and Cs, as well as a negative correlation with Sr, Sc, V, Cr, Cu, Zn, and Co (Tables 1 and 3). The $\delta^{18}O$ values of lavas show a positive correlation with SiO_2 content (Fig. 9), and the high-^{18}O 1943 xenoliths and the basement samples fall close to an extrapolation of the trend line of the Paricutin lavas, whereas the low-^{18}O xenoliths clearly do not. The low-^{18}O xenoliths have higher SiO_2 contents than the

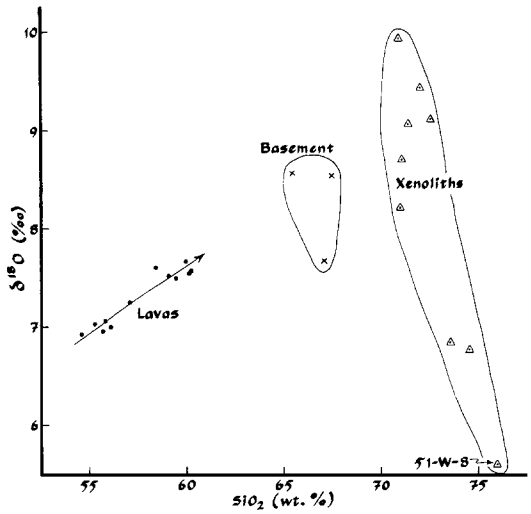

Fig. 9. Plot of $\delta^{18}O$ vs SiO_2 contents of lavas, basement rocks, and xenoliths. Mixing curves are approximately *straight lines* on this type of diagram, because most rocks have very similar bulk oxygen concentrations

others, and in fact the xenolith population as a whole shows a good *negative* correlation between SiO_2 and $\delta^{18}O$. This trend at a high angle to the positive correlation between the lavas and high-^{18}O xenoliths suggests that the low-^{18}O xenoliths are SiO_2-rich partial melts and that the melting process was facilitated by the H_2O-rich, meteoric-hydrothermal environment at the roof of the magma chamber. Note that the lowest-^{18}O, highest-SiO_2, glass-rich xenolith (51-W-8) also has the highest K_2O content and contains by far the most radiogenic Sr (0.7101) of all the samples analysed in this study. It is also poorest in Fe, Mg, Ca, Zr, Li, Ba, Sr, Sc, Zn, La, Ce, and Nd contents of any Paricutin sample. This low-^{18}O xenolith has an atypical "flat" REE pattern (Fig. 6) and plots at extreme positions in the diagrams of Fig. 7. Some of these anomalous chemical effects may be the result of hydrothermal alteration and melting.

Strontium isotopes

Strontium isotopic compositions and Rb and Sr concentrations of lavas, xenoliths, and nearby granodioritic basement rocks are reported in Table 3 and plotted in Figs. 8 and 10.

Lavas

The lavas show no significant change in Sr isotopic composition until more than 80% of the magma had been erupted; $^{87}Sr/^{86}Sr$ remains uniform at 0.7037 to 0.7039 until 1947. Lavas of 1947 and 1952 show significant enrichment in radiogenic Sr, coincident with the increase in $\delta^{18}O$ values (Fig. 8). As the eruption progressed, the $^{87}Rb/^{86}Sr$ ratio rose only moderately (from 0.06 to 0.14) owing to a late rapid doubling of Rb content and small concurrent decrease in Sr (Fig. 5).

The initial $^{87}Sr/^{86}Sr$ ratio of the main body of Paricutin magma, about 0.7038, is in the lower part of the range observed for the Mexican Volcanic Belt (0.7032 to 0.7048) (Moorbath et al. 1978; Verma 1983; Whitford and Bloomfield 1976) and typical of the values observed in volcanoes on normal to thin crust of continental margins or in island arcs (Gill 1981; Hawkesworth 1982). This value could represent a mixture of depleted-mantle-derived strontium and radiogenic crustal strontium either carried into the mantle by subduction or encountered during ascent through the curst. Most likely it is both.

Xenoliths and nearby basement rocks

Except for one of the low-^{18}O samples (51-W-11), the analysed xenoliths approximately fit an isochron for an age of 34.6 ± 1.0 Ma and initial ratio of 0.7043 ± 0.0001 (Fig. 10). The nearby basement samples define a somewhat different isochron of 51 ± 7 Ma with an initial ratio of 0.7034 ± 0.0003 (Fig. 10). It is possible that both of these are real ages. Geochronometric studies of igneous rocks in the Sierra Madre Occidental have shown a bimodal concentration of Cenozoic ages – an early group greater than 45 Ma old and a younger group 34 to 23 Ma old (McDowell and Keizer 1977; McDowell et al. 1978; Clark et al. 1982; Verma 1984). A similar distribution of ages is observed south of the Mexican Belt in the state of Guerrero (R.L. Armstrong and Z. DeCzerna, unpublished data). The different isochrons suggest that the igneous rocks of the upper crust in the Paricutin area could well include rocks of both age groups. In support of this argument, we note, as did Verma (1984) in the Sierra Madre Occidental, a lower initial Sr isotope ratio for igneous rocks older than 45 Ma.

Some of the xenoliths are almost certainly derived from Mid-Tertiary volcanic rocks, largely dacitic and rhyolitic ignimbrites, that are known to underlie the Paricutin region (Wilcox 1954). Similar rocks have initial Sr isotope ratios ranging from about 0.7042 to 0.7050 with a median value of 0.7047 (Lanphere et al. 1980), as well as Sr and Rb contents of 100 to 400 ppm and 70 to 200 ppm, respectively (Cameron and Hanson 1982).

Thus, in contrast to the Paricutin magmas, the xenoliths, Mid-Tertiary volcanic rocks, and basement samples all have more Rb, less Sr, higher Rb/Sr ratios, and, in general, more radiogenic Sr. These are accurately measured numbers, the concentrations showing close agreement with different methods and between different laboratories (Table 3), and they provide a forceful quantitative test for any contamination hypothesis.

Mass-balance calculations

Major elements

Wilcox (1954) calculated the effects of fractionation of olivine and plagioclase and concurrent assimilation of "average" xenolithic material by a graphical method that was later shown to be consistent with a mathematical solution devised by Bryan (1969). Miesch (1979) used a method of vector analysis to examine variations within the same series of analyses and concluded that the compositions evolved through three stages, each of which was represented by a nearly linear compositional trend. The first could be explained by fractionation of olivine and plagioclase, the second by fractionation of Ca-poor pyroxene and plagioclase, and the third by assimilation of granitic wall rocks. The two inflections between the three trends noted by Miesch correspond closely to those shown in the CMAS diagram of Fig. 4.

Least-squares mixing calculations can be used to assess

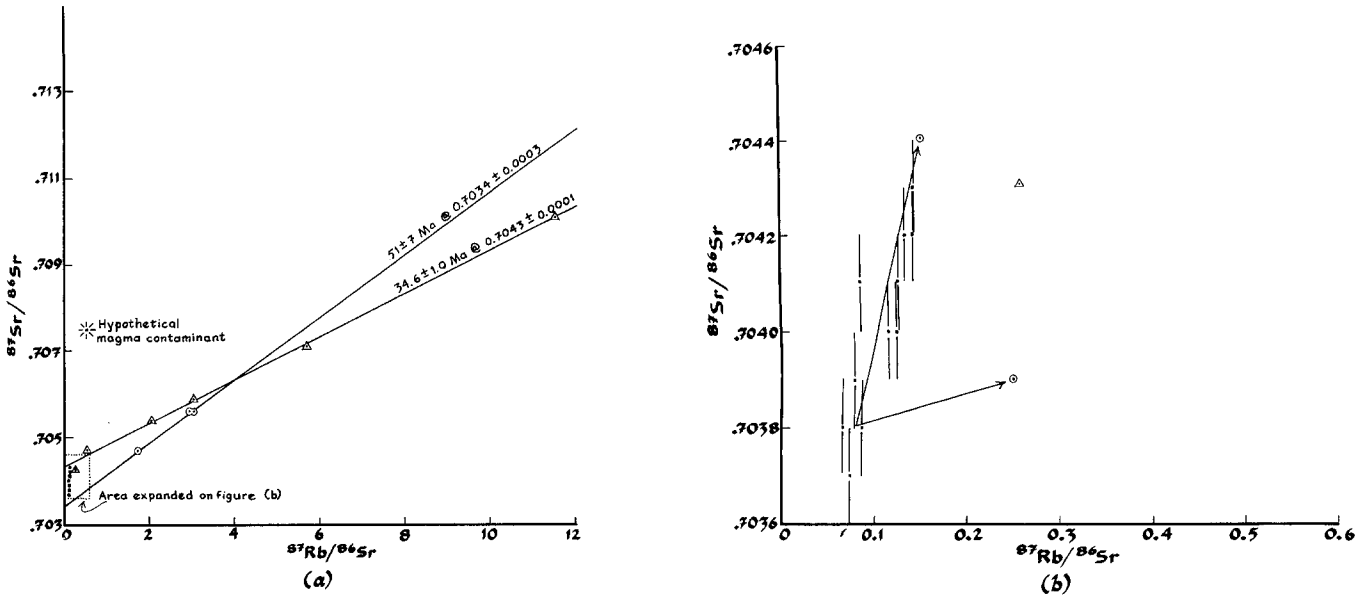

Fig. 10a, b. Rb–Sr isochron diagrams for Paricutin rocks showing the relationships of xenoliths (*triangles*), samples of basement rocks (*circled dots*), and lavas (*dots*). The diagram on the right shows an expanded part of the dashed rectangular area at the lower left of the diagram on the left. Also shown are mixing lines for two possible contaminants. The steep arrow is for the initial magma and 25% of the hypothesized Sr-rich contaminant required by the mass-balance calculations of Fig. 11. The lower arrow is for the initial magma and a contaminant consisting of 25% average xenoliths and granitic basement rocks (lower circled dot)

the effects of assimilating xenoliths while fractionating specific combinations of minerals. Analyses of phenocrysts and xenoliths can be used to determine whether any reasonable combination of these components might explain the variations of major- and trace-elements from one stage of differentiation to another. This has been done for each of the three major segments of the trends shown in Fig. 4.

The first stage has two parts, but the slight difference between them can be explained as the result of a slightly greater proportion of olivine crystallizing from the very earliest lavas. The main trend requires fractionation of plagioclase to explain the reduction of Al_2O_3 and Sr. A somewhat better fit is obtained if a small amount (about 2%) of average xenolithic material is assimilated at the same time.

The over-all trend of this first stage cannot be adequately modelled in terms of fractionation of amphibole and olivine, in a manner consistent with the hypothetical phase diagram in Fig. 4. The main reason for the discrepancy is that the alumina content of the rocks decrease, whereas fractionation of both olivine and amphibole would cause an increase of this component. Addition of xenolithic material does not have a great enough effect to alter this basic limitation.

During the short intermediate interval in which alumina increased slightly (i.e. the middle stage of Fig. 4), the CMAS diagram indicates that amphibole and hypersthene should have been crystallizing, but a better fit is obtained by subtracting hypersthene and plagioclase and adding xenolithic material. In both the early and middle stages, the calculated results are in better agreement with the observed petrographic relations than with the inferred phase relations at elevated pressures.

The greatest compositional changes took place in the final interval represented by the last 20% of the total volume erupted. These abrupt variations can be explained almost entirely as the effect of an addition of xenoliths. A small amount of hypersthene may have crystallized but the mass-balance calculation indicates that only about half of one weight percent of this mineral was fractionated, an insignificant amount in terms of the reliability of the sampling and analytical data.

Comparison of predicted and observed trends

Using the proportions of magma, crystals, and average xenoliths determined from these mass-balance calculations, it is possible to compare the predicted and observed compositions by plotting one against the other, as illustrated in Fig. 11. Although the correlation seems impressive when data for the middle and late stages of differentiation are portrayed in this way, the results are less than perfect. Ba, Zr, and the REE are anomalous. As would be expected, their concentrations increase with differentiation in the series of lavas, but both Ba and Zr have lower concentrations in the xenoliths than in the lavas to which they are thought to have contributed. For these elements, all analysed xenoliths fall far off the trend of differentiation of the lavas (Fig. 7). The anomalously low ^{18}O xenolith, 51-W-8, consistently shows the greatest deviation from the trend of the lavas. Even if Ba and Zr were totally excluded from all crystallizing minerals, the trend of differentiation of the lava would not be consistent with a combination of crystal fractionation and assimilation in the proportions indicated by the mass-balance calculations for major elements.

For several trace elements, the analyzed basement rocks fall closer to the observed trends of the lavas than do the xenoliths (Fig. 7). The contrast between lithophile elements, such as Zr and Li, in the xenoliths and basement rocks is especially conspicuous. Ba falls somewhat off the projected trend of the lavas, and in the case of Rb, the compositions of xenoliths, though scattered, are closer to the trend of differentiation than are the compositions of the basement rocks. This is also true of included elements, especially Co, Zn, and Sc, which have much lower concentrations in the xenoliths than in the basement rocks and are therefore in better accord with the trend of differentiation in the lavas.

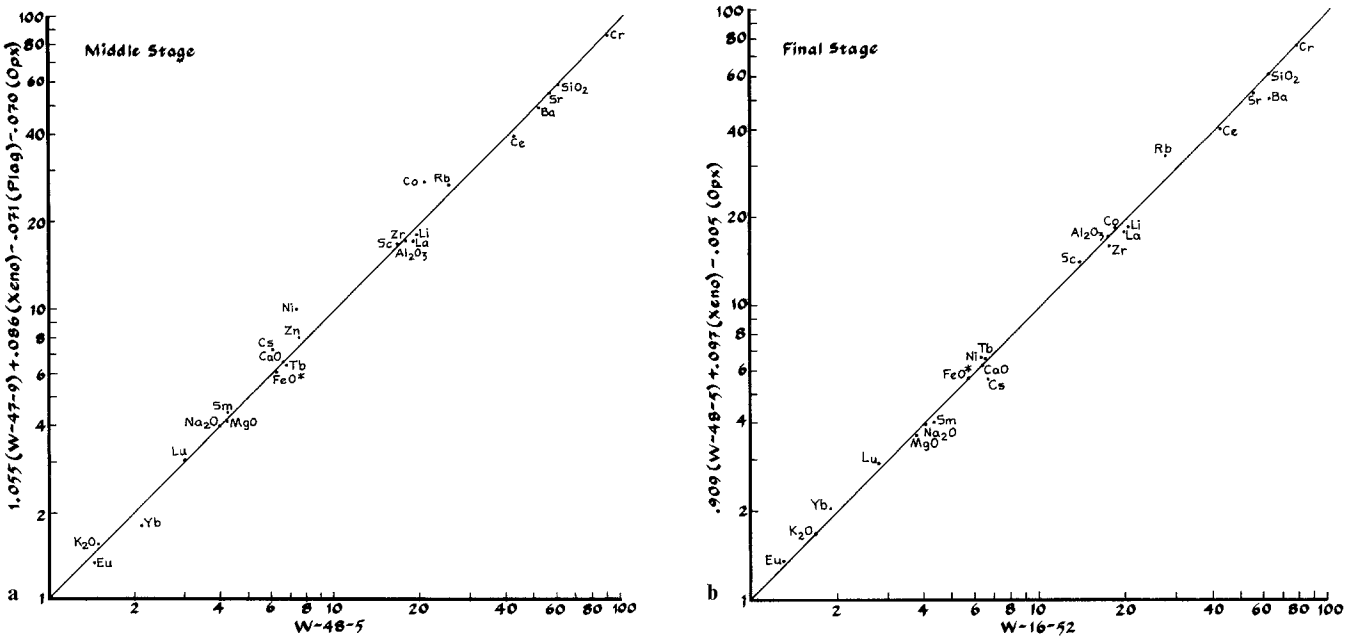

Fig. 11 a, b. Comparison of abundances of elements predicted by mass-balance calculations with those found in rocks presumed to be the daughter products of the differentiation step being tested. Diagram for the middle stage is for differentiation between samples 12 and 16 in Fig. 4, while that for the late stage correspond to samples 16 to 22. Note that some elements, such as Zr, that appear to fit predictions of the mass-balance calculations, do not fit the trends of the variation diagrams in Fig. 7. This is due to the small mass contribution of the xenoliths to the derivative composition and the logarithmic scale on which the components are plotted. Major elements are plotted in weight percent, trace elements in ppm. Ba, Sr, Zr, and Ni are divided by 10, whereas Tb, Cs, and Lu are multiplied by 10. Weighted values used in the mass balance calculations are given in Table 4 together with numerical results

Table 4. Weighted input data and results of mass balance calculations shown in Fig. 11

	Middle stage (W-47-9 to W-48-5)					
	Parent W-47-9	Plag	Opx	Xeno	Daughter W-48-5	Calc. daughter
SiO_2	57.76	53.35	53.86	72.01	58.65	58.67
TiO_2	0.89	0.04	–	0.20	0.77	0.94
Al_2O_3	17.18	29.51	2.46	14.44	17.42	17.29
FeO	6.46	0.93	13.64	1.78	6.06	5.92
MgO	5.61	0.10	28.53	0.89	4.00	4.03
CaO	6.90	11.80	1.48	2.61	6.41	6.65
Na_2O	3.69	4.42	–	3.96	3.89	3.93
K_2O	1.22	0.23	–	3.00	1.49	1.52
P_2O_5	0.29	–	–	0.13	0.30	0.31
R squared = 0.122						

	Late stage (W-48-5 to W-16-5)				
	Parent W-48-5	Xeno	Opx	Daughter W-16-5	Calc. daughter
SiO_2	58.65	72.73	53.65	59.69	59.69
TiO_2	0.77	0.20	–	0.80	0.73
Al_2O_3	17.42	14.58	1.75	17.17	17.17
FeO	6.06	1.80	14.16	5.59	5.66
MgO	4.00	0.90	27.87	3.71	3.66
CaO	6.41	2.63	1.56	6.12	6.09
Na_2O	3.89	4.00	–	3.97	3.90
K_2O	1.49	3.03	–	1.66	1.62
P_2O_5	0.30	0.13	–	0.28	0.28
R squared = 0.022					

The differences between the concentrations of trace elements in the xenoliths and basement rocks suggest that the latter may have gained or lost components as they were reheated and reacted with aqueous fluids in a hydrothermal aureole surrounding the sub-volcanic reservoir. This interpretation is supported by the $\delta^{18}O$ data. Incompatible lithophile elements may have been driven out of inclusions of basement rock and absorbed in the magma, leaving the xenoliths largely depleted of these components. Because we have no way of knowing how closely the samples of nearby basement rocks correspond to the original unaltered compositions of the xenoliths, any further speculation seems unwarranted.

Oxygen isotopes

The oxygen isotope data are compatible with major and trace-element mass-balance calculations. As shown in Fig. 9, the high-^{18}O xenoliths and basement plutonic rocks are both richer in ^{18}O than the initial Paricutin magma, and they would be capable of accounting for the enrichment in ^{18}O in the post-1947 lavas. However, a mixture of 1943 lava ($\delta^{18}O = +6.9$) with basement ($\delta^{18}O = +8.5$) would require assimilation of about 40% of the latter to produce the +7.5 to +7.7 values characteristic of the last 20% of the erupted magma. A more plausible fit is obtained by using the higher-^{18}O xenoliths. With a xenolith of $\delta^{18}O = +9.5$, only about 25% contamination is required.

Following the mass-balance model described above for the major and trace elements (Fig. 11), we start with the measured $\delta^{18}O$ of W-47-9 (+7.25) and find that xenoliths with an average value of +11.2 are required to produce the measured value of +7.59 for W-48-5, if 0.086 is used for the proportion of assimilated material. This value of +11.2 is greater than that of any analysed xenolith; moreover, it is clearly too high, because a continuation of the calculation in Fig. 11 leads to a $\delta^{18}O$ of +7.94 for FP-16-56, 0.3‰ higher than any analysed sample from Paricutin.

Repeating the calculation with $\delta^{18}O = +9.5$ for the xenolithic contaminant, the mass-balance calculation of Fig. 11 gives a plausible $\delta^{18}O$ of +7.44 for W-48-5. Then if we use the 0.097 value from Fig. 11 for the amount of assimilated material ($\delta^{18}O = +9.5$), we also obtain a reasonable value of +7.64 for FP-16-52.

Thus, the general types of calculations for the major and trace elements given in Fig. 11 also give a plausible mass balance for $\delta^{18}O$, if the xenolithic contaminant has a value of about +10.0. However, with a $\delta^{18}O$ value as low as +8.5 (i.e., the highest values observed in the unaltered basement rocks), the fit is poor; values of +7.36 and +7.47 are obtained for W-58-5 and FP-16-52, respectively, and these are lower than the measured values of +7.54 to +7.59.

Strontium isotopes

Although the analysed basement rocks and xenoliths have similar ages and compositions, they cannot be the sole contaminant responsible for the observed Sr isotopic compositions of the late-stage Paricutin lavas; a more radiogenic or more Sr-rich material is required. Figure 12 is a plot of $^{87}Sr/^{86}Sr$ versus 1/Sr; all mixing hyperbolas define straight lines on such a diagram. Except for one low-^{18}O sample, the xenoliths and basement rocks form a nearly linear array that extrapolates toward the late-stage lavas

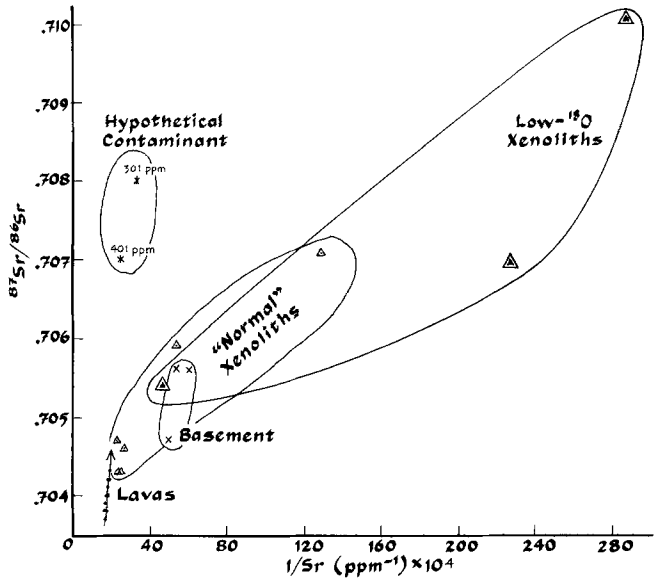

Fig. 12. Plot of $^{87}Sr/^{86}Sr$ vs 1/Sr for the lavas, basement rocks, and xenoliths of Paricutin Volcano. Also shown are the positions of two hypothetical contaminants (containing 401 and 301 ppm Sr) that are required by the mass balance calculations illustrated in Fig. 11. The three low-^{18}O xenoliths, which appear to have been hydrothermally altered, are shown as *large triangles*. Note that mixing curves are *straight lines* on this type of diagram

but is distinct from the trend of the lavas themselves. The arrow indicating the effect of contamination has a much steeper slope (Figs. 10 and 12). Contamination lines calculated using typical xenoliths and basement rocks have lower slopes implying a greater increase in Rb/Sr ratio and a greater decrease in Sr content than is observed in the lavas.

A mixture in equal proportions of initial magma ($^{87}Sr/^{86}Sr = 0.7038$, 17 ppm Rb, 600 ppm Sr) and average xenolith-basement ($^{87}Sr/^{86}Sr = 0.7060$, 150 ppm Rb, 125 ppm Sr) would have an approximate isotopic ratio of 0.7042, but the Rb content of 84 ppm is too great, while the Sr content of 363 is much too low. Mixtures consistent with major-element mass balance calculations would have isotopic ratios of less than 0.7040 and Sr contents much lower than those of the late-stage magmas. For example, the W-47-9 and W-48-5 magmas have identical $^{87}Sr/^{86}Sr$ ratios of 0.7041, consistent with no radiogenic strontium contamination whatever! Nevertheless, if we account for the change in ppm Sr from 580 to 556 solely by assimilation, the contaminant would have to contain 301 ppm Sr with a $^{87}Sr/^{86}Sr$ value of about 0.708 in order to fit the trajectory of the arrow in Fig. 12. Similarly, if we add 0.097 parts xenoliths to W-48-5, as in Fig. 11b, that material would have to contain 401 ppm Sr with a ratio of 0.7070, in order to produce a lava such as FP-16-52 with a ratio of 0.7043 and 541 ppm Sr. These calculated values are plotted in Fig. 12, and the mean value of these "hypothetical contaminants" is also plotted in Fig. 13.

Excluding the three xenoliths in Table 3 that have $\delta^{18}O$ values of +6.8 or less, the other six xenoliths form tight clusters in Figs. 9, 10, and 12, as they do in Fig. 13 where they are designated as the "normal" group of xenoliths. The latter have a mean $\delta^{18}O$ value of +9.1, a mean Sr ratio of 0.7052, and a mean Sr content of 317. The simple dashed mixing curve in Fig. 13 indicates that about 30 to 35% assimilation of such material would be required to

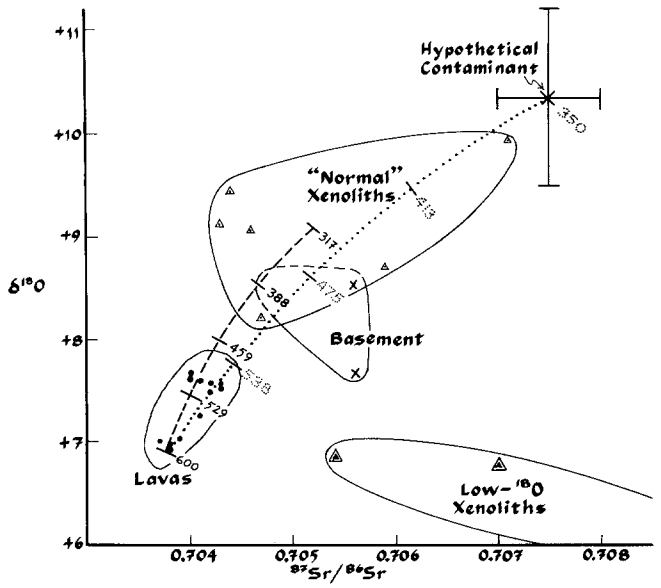

Fig. 13. Plot of $\delta^{18}O$ vs $^{87}Sr/^{86}Sr$ for lavas, xenoliths, and basement rocks. The xenoliths are subdivided into a "normal" group and a low-^{18}O group. Also shown is the hypothetical Sr-rich contaminant with 350 ppm Sr, $^{87}Sr/^{86}Sr = 0.707$ to 0.708, and $\delta^{18}O = +9.5$ to $+11.2$ required by the mass balance calculations of Fig. 11. Two calculated mixing curves show Sr values (in ppm) at the short cross marks corresponding to 75, 50, 25, and 0% contamination of a parental magma represented by the early lavas (600 ppm Sr). The *dashed curve* is for assimilation of the average of six "normal" xenoliths (317 ppm Sr), and the *dotted curve* represents assimilation of the hypothetical contaminant

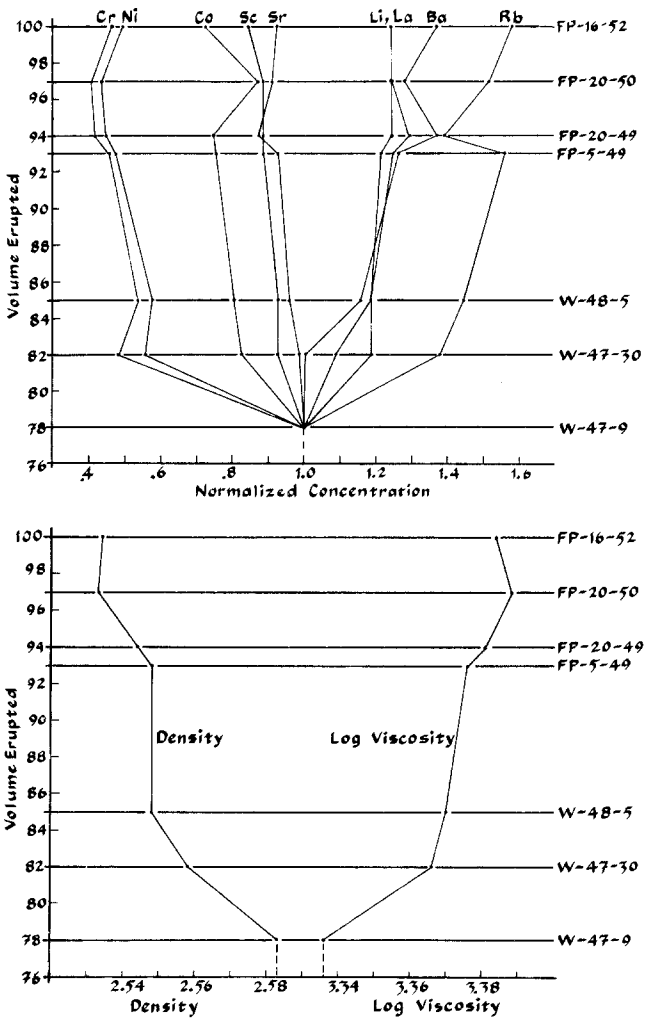

Fig. 14. Variations of included and excluded elements in late stage lavas normalized to concentrations in the latest of the main series of undifferentiated lavas of the earlier stage. Densities for the same lavas have been calculated as liquids at 1,100° C by a method similar to that of Bottinga and Weill (1970) to illustrate the decline of density in the upper levels of a compositionally-graded magma chamber. Note that the abrupt changes of density and trace-elements that took place after about 80% of the total volume had erupted coincide with the equally abrupt changes of isotopes shown in Fig. 8

account for the late-stage lavas, considerably more than the 20% needed to explain most of the major and trace-element data of Fig. 11. However, an overall 20% addition of the "hypothetical contaminant" with a present-day $^{87}Sr/^{86}Sr$ ratio of 0.7075, Rb content of 70 ppm, and Sr content of 350 ppm, and $\delta^{18}O = +10.35$ would yield a mixture with a Sr isotope ratio of 0.7043, 27.6 ppm Rb, 550 ppm Sr, and $\delta^{18}O = +7.6$, very close to the latest magma (Figs. 12 and 13). Such rocks could be a combination of basement rocks, Tertiary volcanic rocks, and some other type of material, such as ancient intermediate crust with an age of about 1 Ga, seawater-altered mafic volcanic rocks, sediment derived from such material, or a variety of marine sediments, such as a Mesozoic limestone-shale mixture. Although the high Ba and low Cr and Co contents of the contaminant implied by the plots of Fig. 7 are consistent with a sedimentary or metasedimentary character, the oxygen isotope ratios are not. Typical unmetamorphosed sedimentary rocks, particularly limestones and shales, have $\delta^{18}O$ values of $+15$ to $+25$, much too high to be compatible with the mass balance discussed in the preceding section. Igneous or metamorphic rocks with $\delta^{18}O$ values of about $+9$ to $+13$ would be more consistent with the oxygen isotope data (Fig. 13). The range of $\delta^{18}O$ values and Sr ratios in the Paricutin lavas, xenoliths, and basement rocks is similar to that observed in the Peninsular Ranges batholith (Fig. 14), where at least three end-member components are required to account for the variations (Taylor and Silver 1978).

The isotopic data indicate some contamination with rocks other than the Cenozoic granitic and volcanic rocks of the local upper crust but similar to average Phanerozoic continental crust in Rb and Sr content and Sr and oxygen isotope ratios. These conclusions are not markedly modified if a more complex assimilation-fractional crystallization model is assumed, because magmatic fractionation of Rb and Sr within the brief eruptive episode is minor and could be responsible, at best, for only a small increase in Rb and a slight decrease in Sr. The minor decrease of Sr and the lack of a Eu anomaly in the lavas appear to rule out major plagioclase fractionation.

Whitford and Bloomfield (1976) observed a steep correlation between Rb/Sr and $^{87}Sr/^{86}Sr$ in lavas from Nevado de Toluca (420 ± 95 Ma lava isochron compared with 403 ± 85 found for the lavas of Paricutin), indicating that Sr isotopic evidence for crustal contamination is not unique to Paricutin. Although Moorbath et al. (1978) and Verma (1983) concluded from their Sr isotopic studies of scattered samples from the Mexican Volcanic Belt that there was no significant sialic contribution to the magmas, evidence for contamination may have been lost in geologic noise

caused by sampling of random lavas rather than a single eruptive sequence. Verma (1984) concluded that the high and variable initial Sr isotope ratios of felsic volcanic rocks of Zacatecas in the Sierra Madre Occidental was due to large amounts of crustal contamination (20 to 85%); we see only the beginning of such wholesale contamination at Paricutin.

Mechanism of differentiation

Certain limitations can be placed on the physical processes responsible for the variations seen in the Paricutin lavas. First, the magma must already have been compositionally zoned in its reservoir prior to the eruption; the nine-year period of activity was too short for the compositional differences to have developed by any known mechanism of differentiation. It is more likely that the magma became zoned in a shallow reservoir before the first discharge of magma in 1943. Studies of the isotopes of radon and lead indicate that the system was probably evolving for at least 50 to 100 years prior to the eruption (Reid 1984).

The geochemical relations show that the chief cause of differention was assimilation of Phanerozoic continental crustal rocks similar in many respects to the rocks seen in outcrops near the edge of the volcanic field. Although crystal fractionation contributed to the compositional variations, especially of the more mafic lavas, it cannot account for the later lavas of more evolved compositions. Wilcox (1954) showed that the amount of crystallization was too limited to have contributed all the heat required to assimilate the basement rocks and that a larger source of heat must have been available. This conclusion is supported by our own studies, which have shown the amount of assimilation to have been even greater than that postulated by Wilcox. The source of additional heat could have been a larger mass of basic magma that remained in the reservoir. According to Scandone (1979), the rate of discharge of magma was directly related to the distribution of thermal energy in the magma and the declining rate of effusion in the last four years reflected the absorption of energy by the process of differentiation.

The model proposed by Wilcox (1954) to explain the evolution of the zoned magma was based on a mechanism of convective stratification proposed by Holmes (1931). It was thought that, as the magma rose through granitic crustal rocks, its upper part became increasingly contaminated and lighter until its density was less than that of the main mass of uncontaminated magma and the two parts of the rising intrusion could no longer convect and mix as a single body. The contaminated magma would have accumulated in a separate zone overlying a much larger mass of denser, hotter magma of more primitive composition. This basic idea has been developed by more recent studies showing that the light contaminated liquid could have been fractionated and ponded under the roof as the intrusion melted its walls (McBirney et al. 1985). Nilson et al. (1985) have examined the behavior of light liquids produced by crystallization or melting at the walls of a mafic intrusion and explained how a buoyant liquid could rise along the walls and accumulate in the upper levels of the reservoir. As it does so, it may back-mix with the more primitive magma, so that the liquid collected under the roof would be compositionally graded. Such a process has been shown to be capable of producing the observed volumes of zoned

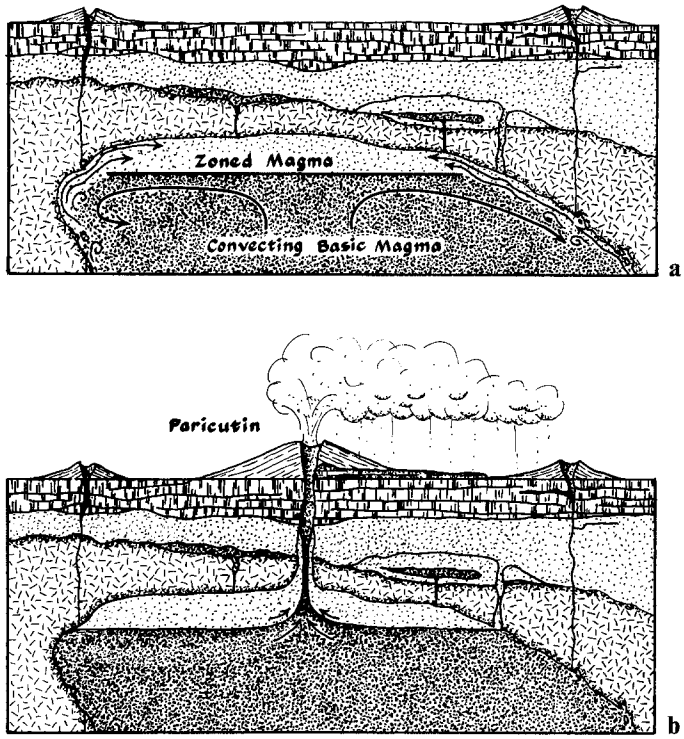

Fig. 15. a Silica-enriched magma resulting from melting and assimilation of crustal rocks in more primitive magma is thought to have formed a buoyant boundary layer that rose and collected under the roof of the reservoir. **b** Tapping of these two zones led to more rapid rise of the denser but less viscous lower magma and later eruption of more silica-rich fraction when the rate of discharge declined

magma in a period of the order of decades to centuries depending on the shape and rate of cooling of the intrusion.

Baker et al. (1985) point out that the variations observed at Paricutin are consistent with those predicted by this interpretation. When the compositions of late-stage lavas are normalized to that of the main mass of less-differentiated early lavas (Fig. 14), they have a pattern similar to that produced by fractionation of liquids by double-diffusive boundary-layer flow. Included elements, such as Cr, Ni, Co, and Sc, are progressively depleted in the later lavas, while lithophile elements, such as Li, the REE, Ba and Rb are enriched. This pattern corresponds to what would be expected if a liquid produced by melting of crustal rocks mixed with the main magma to produce intermediate compositions that rose to find their appropriate density levels in the stratified chamber (Fig. 15).

In order to explain the eruption of lavas in an order that was the reverse of what would be expected if the light differentiated magma were in the upper part of the reservoir, Wilcox (1954, Fig. 107) proposed that the vent tapped the lower flanks of a steep-sided body and drew the magma down in such a way that the last liquid to appear was from the upper-most part of the intrusion. Another explanation for the order of eruption can be deduced from the recent work of Blake (1981), Koyaguchi (1985), and Blake and Ivy (1986). The scheme depicted in the lower part of Fig. 15 requires no special geometrical relations but only a contrast in the densities and viscosities of the two parts of the zoned magma. When magmas with differing properties rise through a channel tapping a compositionally zoned

reservoir, the lower liquid tends to be drawn up and enter the central part of the conduit. If the lower liquid is less viscous, it tends to flow more rapidly and, even though it is denser and starts at a lower level, it can reach the surface before the more viscous differentiated liquid. As the rate of discharge declines, the draw-up diminishes and the lighter more viscous liquid is able to escape without entraining the lower part of the reservoir.

Conclusions

Most of the new geochemical data confirm the original interpretation of the zoned Paricutin lavas as products of extensive assimilation of felsic basement rocks by a magma with a composition of basaltic andesite represented by the earliest lavas. Improved and more detailed calculations of mass-balance relations indicate that the amount of crystal fractionation accompanying assimilation was probably less than originally estimated. Most of the heat required to assimilate the felsic crustal rocks must therefore have come from a larger body of convecting mafic magma at greater depths.

The main mass of magma evolved by fractionation, first of olivine, and then hypersthene, plagioclase, and possibly amphibole. The mineral assemblages in the rocks are in general accord with the phase relations deduced experimentally by Eggler (1972) and Cawthorn and O'Hara (1976) if allowance is made for breakdown of amphibole and loss of water during ascent of the magma from the level where most of the differentiation took place.

Although the general relationships are clearly established, the exact nature and composition of the assimilated material cannot be deduced from the available samples of xenoliths and basement rocks. This may be due in part to the wide diversity of their original compositions and in part to disequilibrium partitioning of components during contact metamorphism, melting, and assimilation. The mechanism responsible for differentiation and zoning was probably one of liquid fractionation in which a contaminated magma of low density was segregated into the upper levels of a shallow chamber. The order of eruption is best explained as the result of withdrawal of liquids of differing densities and viscosities from a compositionally zoned reservoir.

Acknowledgements. We are grateful to Ray E. Wilcox for supplying the critical samples from his original work and for his careful review of the manuscript. Despite our additional data, we have not been able to improve materially on the conclusion he reached more than thirty years ago. Additional samples were supplied by the National Museum of Natural History. Christine McBirney carried out the new major-element analyses and was responsible for most of the trace element determinations. Mrs. Robert Hill performed microprobe analyses of minerals and glasses. Krista Scott assisted with the Rb, Sr, and Sr isotopic analyses. Discussions with B.H. Baker, L.T. Silver, and Harry Flashman have been especially helpful. The work was carried out under NSF Grant No. EAR-7909458 to A.R. McBirney, NSF Grant No. EAR-78-16874 to H.P. Taylor, and Canadian NSERC Grant No. 67-8841 to R.L. Armstrong.

Appendix. Analytical methods

Major and trace elements

Earlier analyses reported by Wilcox (1954) were repeated on material from the same hand specimens and found close to those obtained by atomic absorption and colorimetry in our current work. In order to facilate comparisons of data obtained in different laboratories by different methods of analysis, small systematic differences in SiO_2, CaO, and Na_2O were allowed for by normalizing the new analyses to the original set by means of a weighting factor obtained by repeating the old analyses. In doing so, we may have sacrificed accuracy in the interest of compatible data, without which comparisons of members of the suite would, of course, be impossible. This effect is important only for the major elements of a sample of lava, No. 108081, supplied by the National Museum of Natural History and not included in Wilcox's original suite. Ba, Li, Rb, Cs, Sr, Zn, Cr, Co, Zn, and Cu were measured by atomic aborption, Rb, Sr, Ni, and Zr by x-ray fluorescence, and Sc, Hf, Ta, Th, U, and the REE by neutron activation.

Oxygen isotopes

The $\delta^{18}O$ values were measured by the fluorine extraction technique described by Taylor and Epstein (1962), and are given in parts per thousand (per mil) relative to SMOW (standard mean ocean water); NBS-28 has a $\delta^{18}O$ of $+9.60$ on this scale. The analyses are precise to $+/-0.1$ per mil.

Sr, Rb, and Sr isotopes

Rb and Sr concentrations were determined independently at the University of British Columbia and University of Oregon by replicate analysis of pressed powder pellets using X-ray fluorescence. U.S. Geological Survey rock standards were used for calibration; mass absorption coefficients were obtained from Mo Kα Compton scattering measurements. Rb/Sr ratios have a precision of 2 percent (1 σ) and concentrations a precision of 5 percent (1 σ). Sr isotopic compositions were measured at the University of British Columbia using unspiked samples prepared by standard ion exchange techniques. The mass spectrometer used for the initial work (60° sector, 30 cm radius, solid source) is a U.S. National Bureau of Standards design, modified by H. Faul. Data acquisition is digitized and automated using a NOVA computer. All samples were analyzed in duplicate. Later analyses were carried out by a VG isomass 54R mass spectrometer automated with a HP85 computer. Experimental data have been normalized to a $^{86}Sr/^{88}Sr$ ratio of 0.1194 and adjusted so that the NBS standard $SrCO_3$ (SRM987) gives a $^{87}Sr/^{86}Sr$ ratio of $0.71022+/-2$ and the Eimer and Amend Sr a ratio of $0.70800+/-2$. The precision of a single measurement of $^{87}Sr/^{86}Sr$ ratio is 0.00015 (1 σ) or in the case of the duplicate analyses reported here, 0.0001 (standard error of the mean). Single micromass 54R analyses have a precision of 0.0001 or better. Rb–Sr dates are based on a Rb decay constant of 1.42×10^{-11} y^{-1}. The regressions are calculated according to the technique of York (1967).

References

Anderson AT Jr (1974) Chlorine, sulfur, and water in magmas and oceans. Geol Soc Amer Bull 85:1485–1492

Anderson AT Jr (1979) Water in some hypersthenic magmas. J Geol 87:509–531

Anderson AT Jr, Clayton RN, Mayeda T (1971) Oxygen isotope geothermometry of mafic igneous rocks. J Geol 79:715–729

Blake S, Ivy GN (1986) Density and viscosity gradients in graded magma chambers and their influence on withdrawal dynamics. J Volcanol Geotherm Res, in press

Bottinga Y, Weill DF (1970) Densities of liquid silicate systems calculated from partial molar volumes of oxide components. Am J Sci 272:438–475

Bryan WB (1969) Material balance in igneous rock suites. Carnegie Inst Washington Yearb 67:241–243

Cameron KL, Hanson GN (1982) Rare earth element evidence concerning the origin of voluminous mid-Tertiary rhyolitic ignimbrites and related rocks, Sierra Madre Occidental, Chihuahua, Mexico. Geochim Cosmochim Acta 46:1489–1504

Cawthorn RG, O'Hara MJ (1976) Amphibole fractionation in calc-alkaline magma genesis. Am J Sci 276:309–329
Clark KF, Foster CT, Damon PE (1982) Cenozoic mineral deposits and subduction-related magmatic arcs in Mexico. Geol Soc Am Bull 83:533–544
Criss RE, Taylor HP Jr (1983) An $^{18}O/^{16}$ and D/H study of Tertiary hydrothermal systems in the southern half of the Idaho Batholith. Geol Soc Am Bull 94:640–663
Eggler DH (1972) Water-saturated and undersaturated melting relations in a Paricutin andesite and an estimate of water content in the natural magma. Contrib Mineral Petrol 34:261–271
Fries C Jr (1953) Volumes and weights of pyroclastic material, lava, and water erupted by Paricutin Volcano, Michoacan, Mexico. Trans Am Geoph Union 34:603–616
Garlick GD (1966) Oxygen isotope fractionation in igneous rocks. Earth Planet Sci Lett 1:361–368
Gill J (1981) Orogenic andesites and plate tectonics. Springer, Berlin Heidelberg New York, p 390
Hawkesworth CJ (1982) Isotope characteristics of magmas erupted along destructive plate margins. In: Thorpe RS (ed) Andesites. John Wiley & Sons, Chichester, pp 549–571
Holmes A (1931) The problem of the association of acid and basic rocks in central complexes. Geol Mag 68:241–255
Koyaguchi T (1985) Magma mixing in a conduit. J Volcanol Geotherm Res 25:365–369
Krauskopf KB (1948) Mechanism of eruption of Paricutin Volcano, Mexico. Geol Soc Am Bull 59:711–731
Lanphere MA, Cameron KL, Cameron M (1980) Sr isotope geochemistry of voluminous rhyolitic ignimbrites and related rocks, Western Mexico. Nature 286:594–596
Masi U, O'Neil JR, Kistler RW (1981) Stable isotope systematics in Mesozoic granites of central and northern California and southwest Oregon. Contrib Mineral Petrol 76:116–126
Matsuhisa Y (1979) Oxygen isotopic compositions of volcanic rocks from the East Japan island arcs and their bearing on petrogenesis. J Volcanol Geotherm Res 5:271–296
McDowell FW, Duex TW, Henry CD, Long LE (1978) Age and strontium isotope chemistry of the Sierra Madre Occidental volcanic province, western Mexico. US Geol Surv Open-File Rpt 78-701:289–291
McDowell FW, Keizer RP (1977) Timing of mid-Tertiary volcanism in the Sierra Madre Occidental between Durango City and Mazatlan, Mexico. Geol Soc Am Bull 88:1479–1487
Miesch AT (1979) Vector analysis of chemical variations in the lavas of Paricutin Volcano, Mexico. Math Geol 11:345–371
Moorbath S, Thorpe RS, Gibson IL (1978) Strontium isotope evidence for petrogenesis of Mexican andesites. Nature 271:437–439
Osborn EF, Rawson SA (1980) Experimental studies of magnetite in calc-alkaline rocks. Carnegie Inst Washington Yearb 79:281–285
Reid MR (1984) Isotopic and trace element geochemistry of Paricutin Volcano: anatomy of crustal assimilation. Proc Conf on Open Magmatic Systems 133–134
Scandone R (1979) Effusion rate and energy balance of Paricutin eruption (1943–1952), Michoacan, Mexico. J Volcanol Geotherm Res 6:49–59
Taylor HP Jr (1968) The oxygen isotope geochemistry of igneous rocks. Contrib Mineral Petrol 19:1–71
Taylor HP Jr (1977) Water/rock interactions and the origin of H_2O in granitic batholiths. J Geol Soc London 133:509–558
Taylor HP Jr, Epstein S (1962) Relationship between $^{18}O/^{16}O$ ratios in coexisting minerals in igneous and metamorphic rocks, Part 1. Principles and experimental results. Geol Soc Am 73:461–480
Taylor HP Jr, Silver LT (1978) Oxygen isotope relationships in plutonic igneous rocks of the Peninsular Batholith, southern and Baja California. US Geol Surv Open-File Rpt 78-701:423–427
Tilley CE, Yoder HS Jr, Schairer JF (1968) Melting relations of igneous rocks. Carnegie Inst Washington Yearb 66:450–453
Verma SP (1983) Magma genesis and chamber processes at Los Humeros Caldera, Mexico – Nd and Sr isotope data. Nature 302:52–55
Verma SP (1984) Sr and Nd isotopic evidence for petrogenesis of mid-Tertiary felsic volcanism in the mineral district of Zacatecas, Zac. (Sierra Madre Occidental), Mexico. Isotope Geosci 2:37–53
Whitford DJ, Bloomfield K (1976) Geochemistry of Late Cenozoic volcanic rocks from the Nevado de Toluca area, Mexico. Carnegie Inst Washington Yearb 75:207–213
Wilcox RE (1954) Petrology of Paricutin Volcano, Mexico. US Geol Surv Bull 965-C:281–353
Williams H (1950) Volcanoes of the Paricutin region. US Geol Surv Bull 965-B:165–279
Yoder HS Jr (1969) Calc-alkaline andesites: experimental data bearing on the origin of their assumed characteristics. Proc Andesite Conf, McBirney AR (ed). Oregon Dept Geol Mineral Ind Bull 65:77–89
York D (1967) The best isochron. Earth Planet Sci Lett 2:479–482
York D (1969) Least squares fitting of a straight line with correlated errors. Earth Planet Sci Lett 5:320–324

Received July 25, 1985 / Accepted September 22, 1986